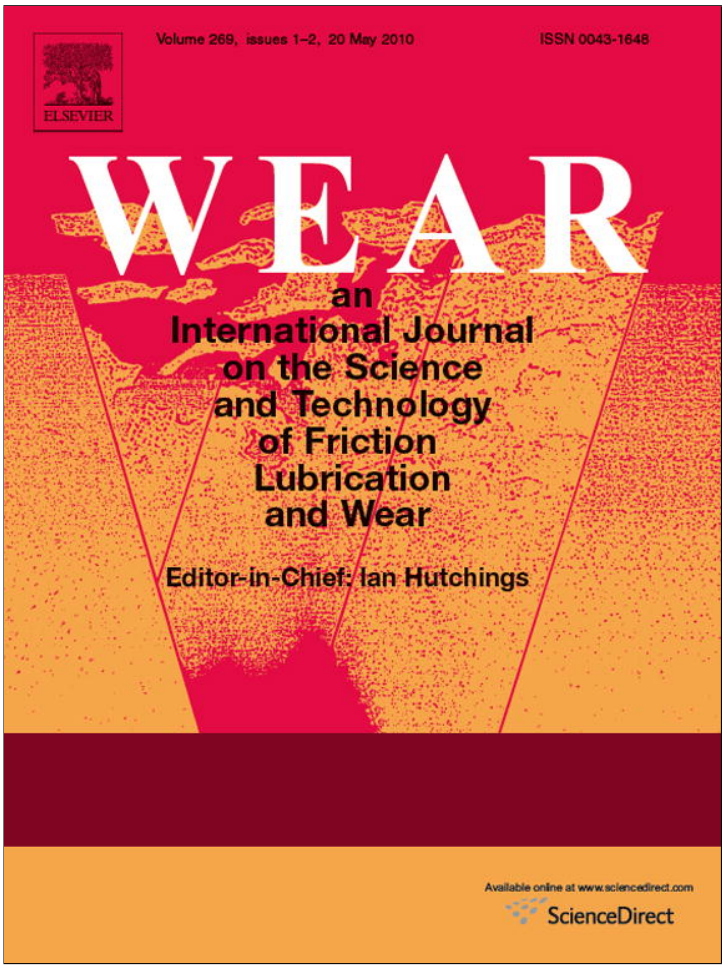

Wear 269 (2010) 71–78

Contents lists available at ScienceDirect

Wear

journal homepage: www.elsevier.com/locate/wear

Wear resistant properties of multi-walled carbon nanotubes reinforced Al_2O_3 nanocomposites

I. Ahmad, A. Kennedy, Y.Q. Zhu*

Division of Materials, Mechanics and Structure, Faculty of Engineering, The University of Nottingham, University Park, Nottingham NG7 2RD, UK

ARTICLE INFO

Article history:
Received 25 June 2009
Received in revised form 5 March 2010
Accepted 10 March 2010
Available online 18 March 2010

Keywords:
Al_2O_3
Carbon nanotubes
Nanocomposites
Tribology
Wear

ABSTRACT

Various amounts of well-dispersed multi-walled carbon nanotubes (MWCNTs) were used to reinforce an Al_2O_3 via a hot-press consolidation. Ball-on-disk wear tests were performed under different loading conditions of 14 N, 25 N and 35 N, to evaluate the wear and tribological properties of the Al_2O_3–MWCNT nanocomposites. In comparison with the monolithic Al_2O_3, the addition of MWCNTs decreased the coefficient of friction in Al_2O_3–MWCNT nanocomposites and a promising 80% reduction in coefficient of friction was recorded for nanocomposite containing 10 wt% MWCNTs, under a sliding load of 14 N. Abrasive sliding wear mechanism was observed in all samples. The results show that additions of MWCNTs can upgrade the monolithic Al_2O_3 and convert it into a wear resistance material. The MWCNTs played dual roles in improving the tribological performance of the nanocomposites, indirectly by influencing the microstructure and mechanical properties of nanocomposites and directly by acting as a lubricating medium.

1. Introduction

Carbon nanotubes (CNTs) are the most intriguing materials for the development of sophisticated engineering materials for advanced applications and large amounts of efforts have been focused on this research frontier [1]. In particular, their exceptional mechanical and outstanding functional characteristics make them suitable candidates as a reinforcement to improve toughness for brittle ceramics and glasses and to increase stiffness and strength for weaker materials such as polymers [2]. To date, intensive research has been reported regarding enhancing the fracture toughness of ceramics matrices [3,4], however less attention was paid to explore their potential tribological features. Because of the closed tubular structure of a graphene sheet, CNTs are expected to form the desired weak interaction with the contacting couple during wear process [5]. In fact, atomistic simulations have predicted that CNTs have the capability to endure significant compressive and tensile forces prior to failure because of their flexibility and high mechanical properties, via a combination of sliding and rolling in response to shear forces [6]. This has been partly validated experimentally when copper matrix was reinforced with CNTs [7], whist reduced wear rate and a stable friction of coefficient was achieved under different loading conditions for carbon/carbon nanocomposites [8]. CNT-reinforced Al_2O_3 nanocomposites have been described previously, focusing on the effects of CNTs on the mechanical properties and electrical performance [9–13], some tribological properties of CNTs reinforced ceramics nanocomposites have been reported, and significant reduction in wear volume with increasing CNTs concentration has also been reported [14–16]. However, in-depth understanding for the tribological performance of Al_2O_3–CNT nanocomposites requires further research.

In this paper, the wear properties of Al_2O_3–MWCNT nanocomposites with various MWCNT contents, under various sliding loads, are presented. Excellent low wear rate has been achieved, and the wear mechanism has been discussed.

2. Experimental procedure

2.1. Materials and characterisation techniques

MWCNTs (Ø ~ 40 nm), as shown in Fig. 1, were well-dispersed within Al_2O_3 nanopowder by practicing unique dispersion method and consolidated by hot-pressing, as described previously [17,18]. In this way, Ø 32 mm × 3 mm discs of Al_2O_3–MWCNT nanocomposites containing various amounts of MWCNTs (0 wt%, 2 wt%, 5 wt% and 10 wt%) were finally prepared. Archimedes method was adopted to measure the densities of samples using theoretical density of 3.99 g/cm^3 and 1.85 g/cm^3 for Al_2O_3 and MWCNTs, respectively. Mechanical properties such as elastic modulus, hardness, fracture toughness and flexural strength of the samples were evaluated using standard testing methods and the general mechanical properties of the samples used in this study are summarised

* Corresponding author. Fax: +44 1159513800.
E-mail address: yanqiu.zhu@nottingham.ac.uk (Y.Q. Zhu).

0043-1648/$ – see front matter © 2010 Elsevier B.V. All rights reserved.
doi:10.1016/j.wear.2010.03.009

Table 1
General structural and property data of the monolithic Al_2O_3 and the MWCNT-reinforced Al_2O_3 nanocomposites used in this study.

Material	Relative Density (%)	Grain size (μm)	Hardness vickers (H_V) (GPa)	Fracture[a] toughness (K_{IC}) (MPa $m^{1/2}$)	Flexural strength (σf) (MPa)	Elastic modulus (E) (GPa)
Monolithic Al_2O_3	97.42	1.3 ± 0.1	16.0 ± 0.4	3.0 ± 0.2	357 ± 27	392 ± 3
Al_2O_3–2 wt% MWCNTs	96.89	0.45 ± 0.02	18.1 ± 0.2	4.3 ± 0.3	380 ± 18	378 ± 5
Al_2O_3–5 wt% MWCNTs	94.17	0.37 ± 0.04	14.8 ± 0.5	4.5 ± 0.2	280 ± 7	291 ± 4.5
Al_2O_3–10 wt% MWCNTs	92.69	0.39 ± 0.06	6.2 ± 0.3	3.9 ± 0.2	245 ± 15	216 ± 3.7

[a] Measured by direct crack measurement (DCM) method.

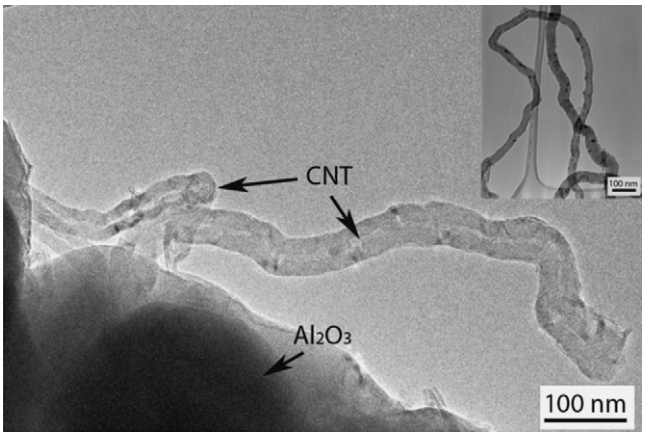

Fig. 1. TEM image of the MWCNT acquired from sintered nanocomposites. Inset shows the raw MWCNTs used to reinforce the Al_2O_3.

in Table 1 [19,20]. Structural features of the fractured surfaces and worn surfaces samples were examined using SEM (Philips/FEI XL30-JEOL 6400). Grain size of the samples was determined by using X-ray diffraction (XRD) technique. For interfacial investigations, transmission electron microscopy (TEM, JEOL 2000 FX and 2100 F) was used and samples for TEM were prepared by utilising focused ion beam scanning electron microscope (FIB-SEM) technique.

2.2. Wear testing technique

The friction and wear experiments were performed by using a ball-on-reciprocating flat geometry [14,15]. A Si_3N_4 ball of Ø 9.8 mm (Dejay Ltd., UK) was used against the pre-polished flat sample surfaces. The tests were performed at different sliding loads (14 N, 25 N and 35 N), at a fixed sliding speed of 10 mm/s with a reciprocating stroke of 10 mm and duration of 120 min. The friction force transferred to a load cell was recorded throughout the tests. The cross-sectional areas of wear tracks of the samples were measured using a TALYSURF CLI 1000 profilometer (Taylor/Hobson

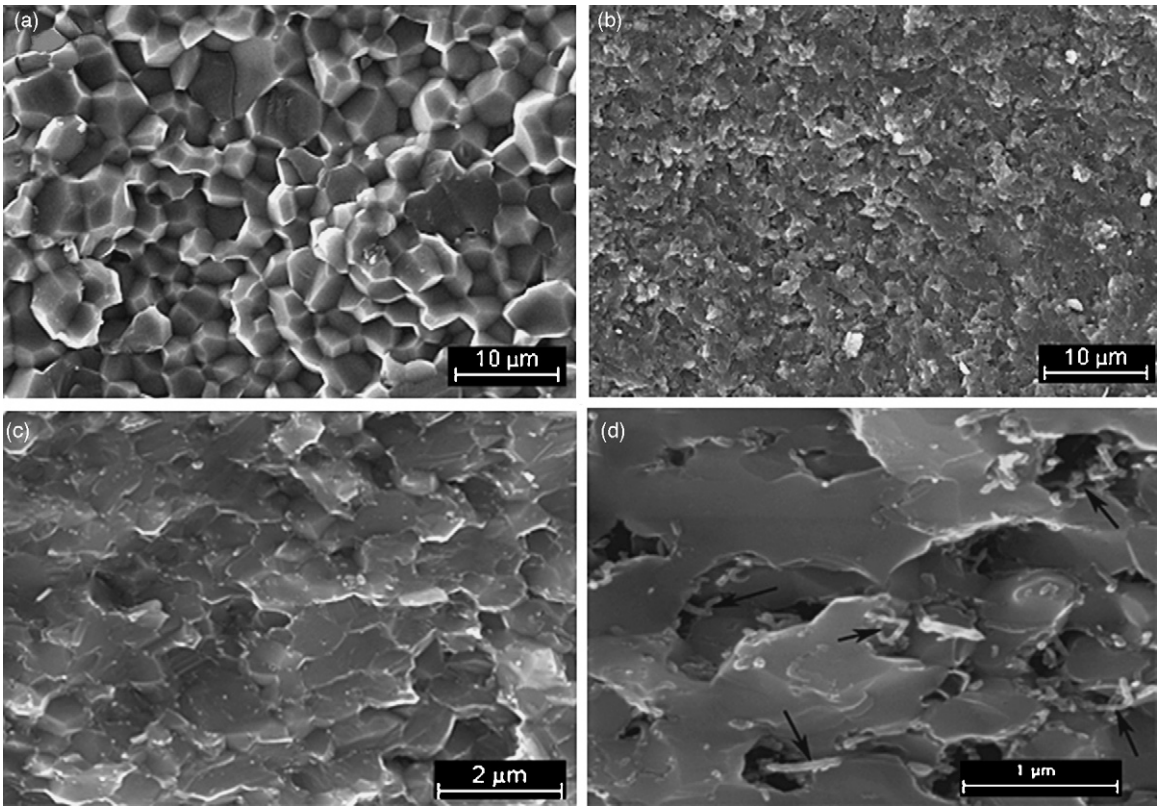

Fig. 2. SEM images of the nanocomposites used in the wear test. (a) Larger/uneven grain size and inter-granular fracture mode in monolithic Al_2O_3, (b) grain refinement and trans-granular fracture in Al_2O_3–MWCNT nanocomposite, (c) demonstration of trans-granular fracture mode at higher magnification, and (d) dispersion of MWCNTs (marked by black arrows) within the matrix.

Precision, UK) and the volume losses of the samples were calculated with the help of attached TalyMap Universal software. Then the specific wear rates were calculated employing Eq. (1) [21]:

$$W = \frac{V}{LF} \quad (1)$$

where L is the sliding distance, F is the applied load, and V the wear volume.

3. Results

3.1. Structural features

Fig. 2 shows the general morphological features of different samples. Fig. 2d is evident that uniform dispersion of MWCNTs within the Al_2O_3 matrix has been obtained and individually dispersed MWCNTs can be identified easily. The additions of MWCNT in Al_2O_3 sharply reduced the grain size by restricting the grain growth, as shown in Fig. 2b. A change in the fracture mode from inter-granular in monolithic Al_2O_3 in Fig. 2a to transgranular fracture in Fig. 2c can also be observed.

3.2. Tribology and wear depiction

Fig. 3a shows the variation in weight loss as a function of MWCNT contents at various sliding loads. A significant reduction in weight loss was observed with increased MWCNT addition, when tested at a specific sliding load. For example, a 14 N sliding load is subject to 35%, 47% and 63% reductions, and for 25 N, 47%, 66% and 86% reduction in weight loss were observed for nanocomposites containing 2 wt%, 5 wt% and 10 wt% MWCNTs, respectively, compared with the monolithic Al_2O_3 tested under similar experimental conditions.

Furthermore, when the sliding load was increased to 35 N, similar trends were found for 2 wt% and 5 wt% MWCNT additions which exhibited 34% and 40% drops in weight loss, respectively. However, an increase in weight loss (43%) was detected at 10 wt% MWCNT addition, compared with monolithic Al_2O_3. A low sliding load (14 N) resulted in 2%, 21% and 80% drops in friction coefficient, and a moderate sliding load (25 N) resulted in 4%, 16% and 44% drops in friction coefficient for the nanocomposites with 2 wt%, 5 wt% and 10 wt% MWCNT additions, respectively, when compared with monolithic Al_2O_3. For high sliding loads (35 N) negligible differences in coefficient of friction were found for those containing 2 wt% and 5 wt% MWCNTs, however the nanocomposite with 10 wt% MWCNTs led to a 19% drop in coefficient of friction, as shown in Fig. 3b. The lowest value for the coefficient of friction (0.11) was observed for 14 N sliding loads for a Al_2O_3–10 wt% MWCNTs nanocomposite and was recorded only 1/4 of the monolithic Al_2O_3 (0.46), when tested under similar experimental conditions.

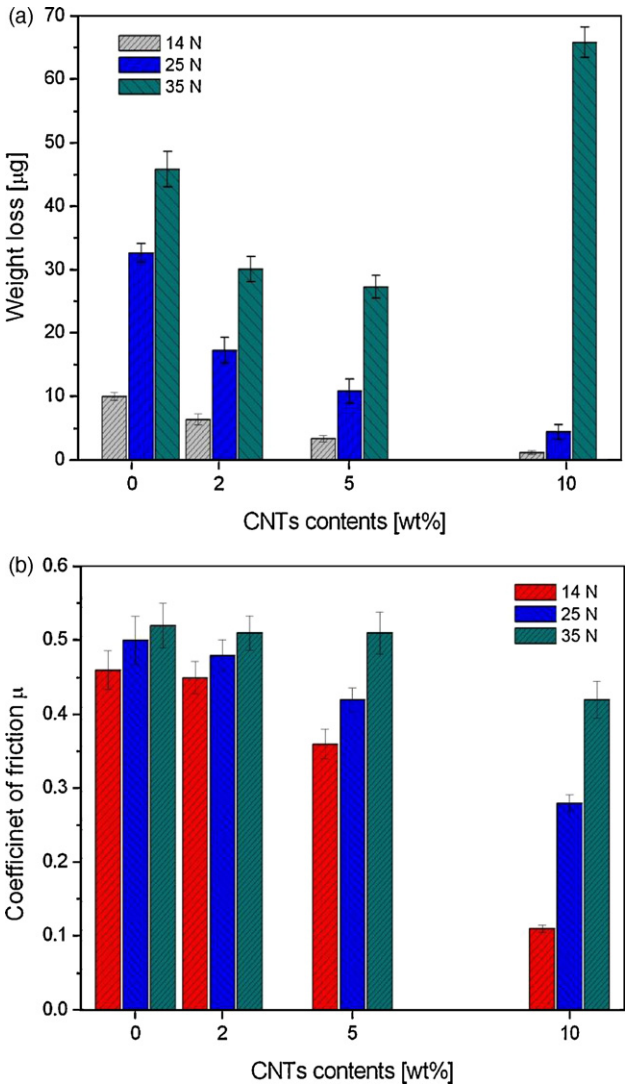

Fig. 3. Effects of MWCNT content on (a) the weight loss and (b) coefficient of friction for Al_2O_3 and the composites tested at various loading conditions.

4. Discussion

4.1. Indirect role of the MWCNTs on tribology and wear of the nanocomposites

4.1.1. Influence of mechanical properties

Wear in ceramic materials is closely attributed to the mechanical properties of the ceramics. Therefore, we can assess the nanocomposite wear performance using their mechanical properties data, in order to gain better understanding as to whether the improved wear resistance is due to the mechanical properties of nanocomposites or arises from other factors [22]. Theoretically, the wear volume of an Al_2O_3–MWCNT nanocomposite can be calculated by employing Evan's formula, Eq. (2) [23]:

$$V = a\frac{F^{9/8}}{K_{IC}^{1/2}H^{5/8}}\left(\frac{E}{H}\right)^{4/5}L \quad (2)$$

where V is the wear volume, F is the applied load, K_{IC} the fracture toughness, H the hardness, a is the constant independent of materials type, and L the sliding distance.

The wear rate ratios obtained experimentally and using Eq. (2) (theoretically) were determined for the nanocomposites by dividing the corresponding wear rate for monolithic Al_2O_3, and are plotted against MWCNT contents in Fig. 4. Varying the loads exhibited little influence on the wear rate ratios (W^c) obtained using Evan's formula. However, reductions in the wear rates for 2 wt% and 5 wt% MWCNT additions and an increase for the 10 wt% MWCNT additions are resulted, as shown in Fig. 4d. This result indicates that the good mechanical properties for nanocomposites containing 2 wt% and 5 wt% MWCNTs are in consistent with their improved wear resistance, and conversely the mechanically weak nanocomposites (10 wt% MWCNTs) exhibit poor wear resistance. In contrast, the wear rate ratios (W^e) calculated based on experimental data are gradually decreased with increasing MWCNT contents under sliding loads of 14 N and 25 N, as illustrated in Fig. 3a and b, except from the 10 wt% MWCNTs sample tested at 35 N, Fig. 4c.

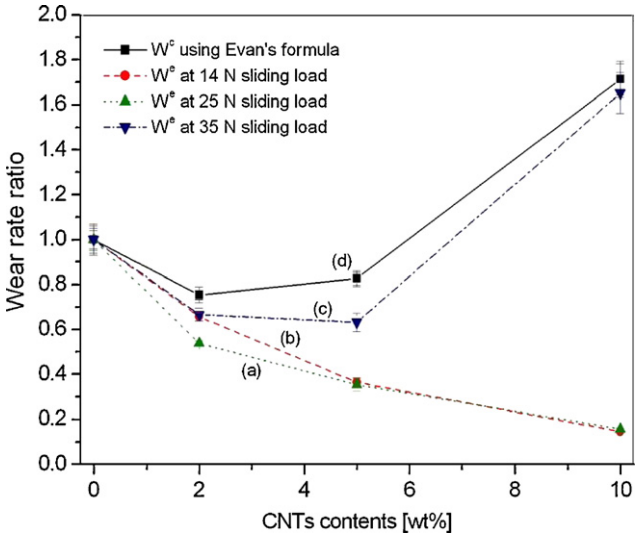

Fig. 4. Effects of MWCNT contents on the wear rate, experimentally determined (W^e) at different sliding loads (a) 14 N, (b) 25 N, (c) 35 N and (d) calculated theoretically (W^c) employing Evan's formula for similar loads.

Based on the wide variations in the wear rates results, calculated theoretically and obtained experimentally for 2 wt% and 5 wt% MWCNTs, it seems that the change of the mechanical properties may not be the main reason for the improved wear resistance of nanocomposite, and that other factors are of importance.

4.1.2. Structural features and wear mechanism

A typical SEM micrograph of the surfaces of the Al_2O_3 and nanocomposite samples after wear testing displays scratches, suggesting an abrasive sliding wear mechanism, as shown in Fig. 5a and b. Close inspection of the worn surface of monolithic Al_2O_3, shown in Fig. 6a, clearly displays microchipping, which can be associated with the inter-granular fracture along the grain boundaries, where pull out of a whole grain is frequently visible (shown by the white arrow). Similar inter-granular fracture features were also identified in fractured samples of monolithic Al_2O_3, as displayed in Fig. 2a.

Much smaller and fewer grain pull-outs and smooth appearance of worn surfaces were observed in the nanocomposites (Fig. 6b–d), compared with monolithic Al_2O_3. Such structural changes may arise from the change in fracture modes and the fine grain structure of the nanocomposites, verified in the fractographs of nanocomposite in Fig. 2b and c. Reported case argued that both these features led to nanocomposite to higher wear resistance [24]. Shallow abrasive grooves on the worn surface of Al_2O_3 and nanocomposites samples, shown in Fig. 6, suggest a deformation-controlled wear mechanism, which is a characteristic of Al_2O_3 under mild wear conditions [25]. The worn surface of nanocomposite samples, as shown in Fig. 6b and c, have a smooth surface in contrast to the monolithic Al_2O_3. These grooves indicate the presence of hard particles during the course of wear. During wear, when two bodies move relative to each other, plastic deformation occurs due to the plowing of asperities on the wear surface. Once the friction induced strain exceeds the limit held by the strength of bonding between the asperities and the substrate, the asperities may break down to form scattered debris and the hardness and morphology of the debris then governs the wear mechanism.

A load dependent wear transition is also evident from the surface texture of worn surfaces, as shown in Fig. 6d, where the nanocomposite exhibits shallow grooves when tested at 25 N loads and much deeper and wider grooves are visible for the same nanocomposite tested under a 35 N loads, Fig. 6a. This morphological change in the groove is associated with the drastic increase

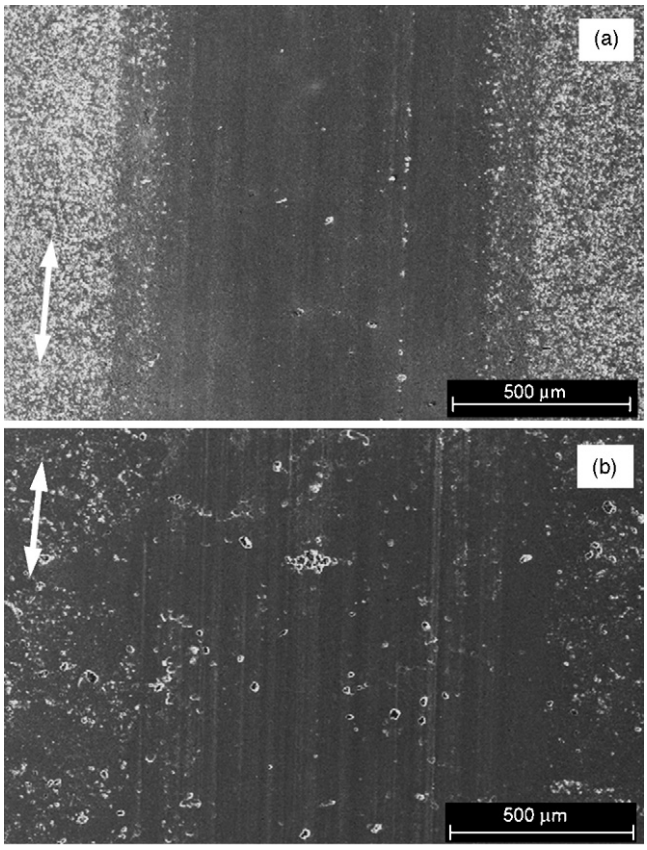

Fig. 5. SEM micrographs of wear tracks occurred on (a) Al_2O_3 and (b) Al_2O_3–MWCNT nanocomposite (white arrows show the sliding direction).

in weight loss (as shown in Fig. 3a), hence associated with the low density and low hardness, as summarised in Table 1. EDX analysis of the worn surface of the samples shown in Fig. 7b has revealed no change in the chemical composition however, the area marked by black arrow was consists of MWCNT agglomerates (Fig. 7c).

Meanwhile, debris collected from the worn surface of monolithic Al_2O_3 and nanocomposites samples revealed a similar chemical composition, as shown in Fig. 8d. Based on the morphology (Fig. 8a) and EDX analysis (Fig. 8d), the debris produced during the wear of monolithic Al_2O_3 was identified as mixtures of Si_3N_4 and Al_2O_3 particles, which further confirmed the two body abrasive wear mechanism. Even though the hardness of the counterpart, Si_3N_4 ball, is much higher (>20 GPa) than monolithic Al_2O_3. It is believed that the Si_3N_4 debris was produced by an abrasive and fatigue wear mechanism [7]. In case of nanocomposites, mild wear at low sliding loads (25 N) produced fine abrasive chippings and short flakes debris (Fig. 8b), and at high sliding loads (35 N) produced wider and thicker flakes, indicating more severe wear conditions. It is clear that the hard debris will increase the wear rate and coefficient of friction in the nanocomposites, and that the presence of MWCNTs must have played a crucial role during the process.

4.2. Direct contribution of the MWCNTs on tribology and wear of the nanocomposites

MWCNTs could make a direct contribution to improving the wear resistance and reducing the friction coefficient in the nanocomposites. In monolithic Al_2O_3, cracks generated during the wear process resulted in pull-out of the whole grain and led to the higher wear rates. In the nanocomposite, MWCNTs presented at the grain boundaries locked the crack propagation and also

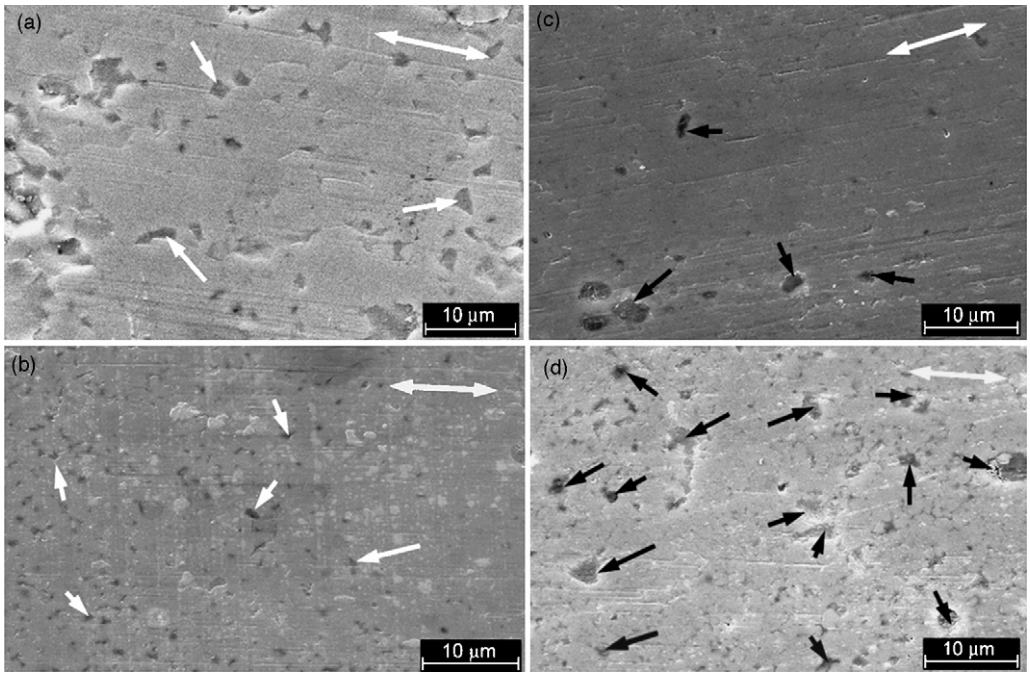

Fig. 6. SEM images of the worn surface (a) monolithic Al_2O_3 (white arrows indicate grain pull-outs), (b) 2 wt% nanocomposite (white arrows indicate grain pull-outs), (c) 5 wt% nanocomposite (black arrows show MWCNTs agglomerates), and (d) 10 wt% nanocomposite, tested at 25 N sliding loads (black arrows show MWCNTs agglomerates). The double head white arrows indicate sliding directions.

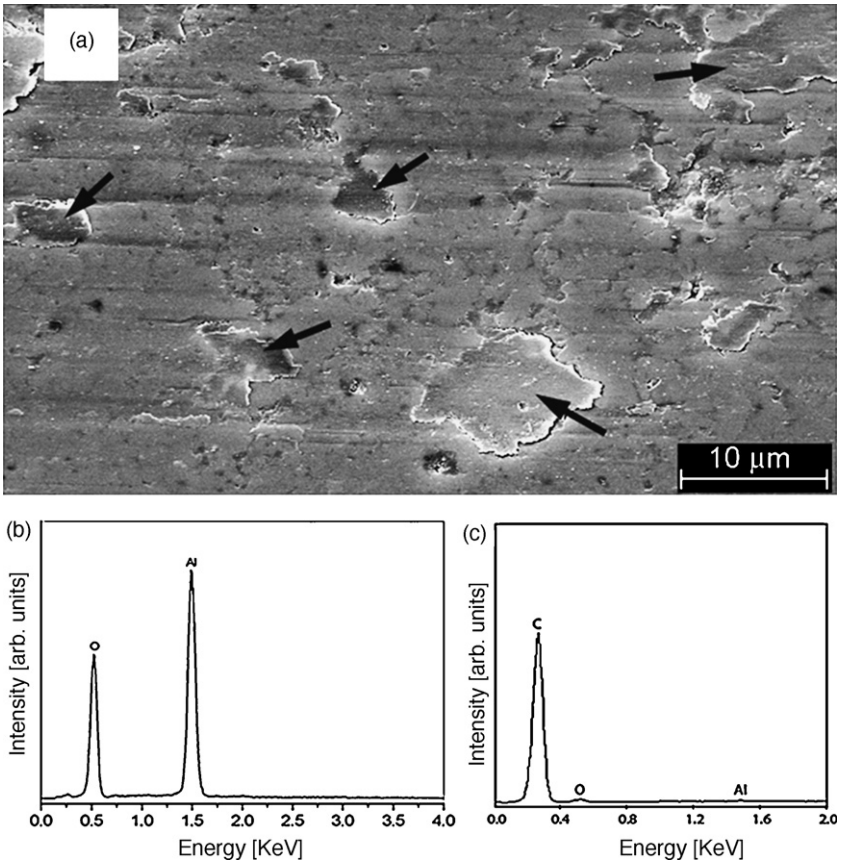

Fig. 7. (a) SEM image of a worn surface of the Al_2O_3–10 wt% MWCNT nanocomposites tested at 35 N sliding loads (black arrow shows flattened MWCNT agglomerates), (b) and (c) EDX profiles of the worn surface and MWCNT agglomerates, respectively.

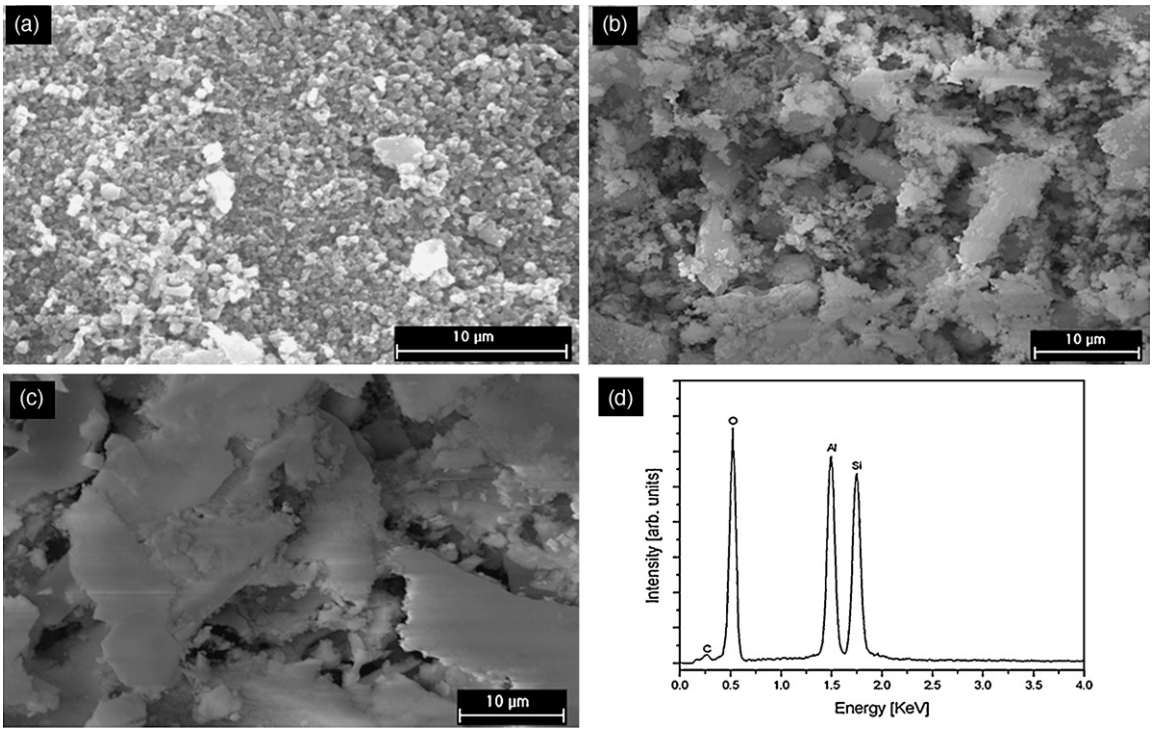

Fig. 8. SEM images of the debris (a) monolithic Al_2O_3, (b) Al_2O_3–10 wt% MWCNT nanocomposites at 25 N sliding loads, (c) Al_2O_3–10 wt% MWCNT nanocomposites at 35 N sliding loads and (d) EDX result of debris.

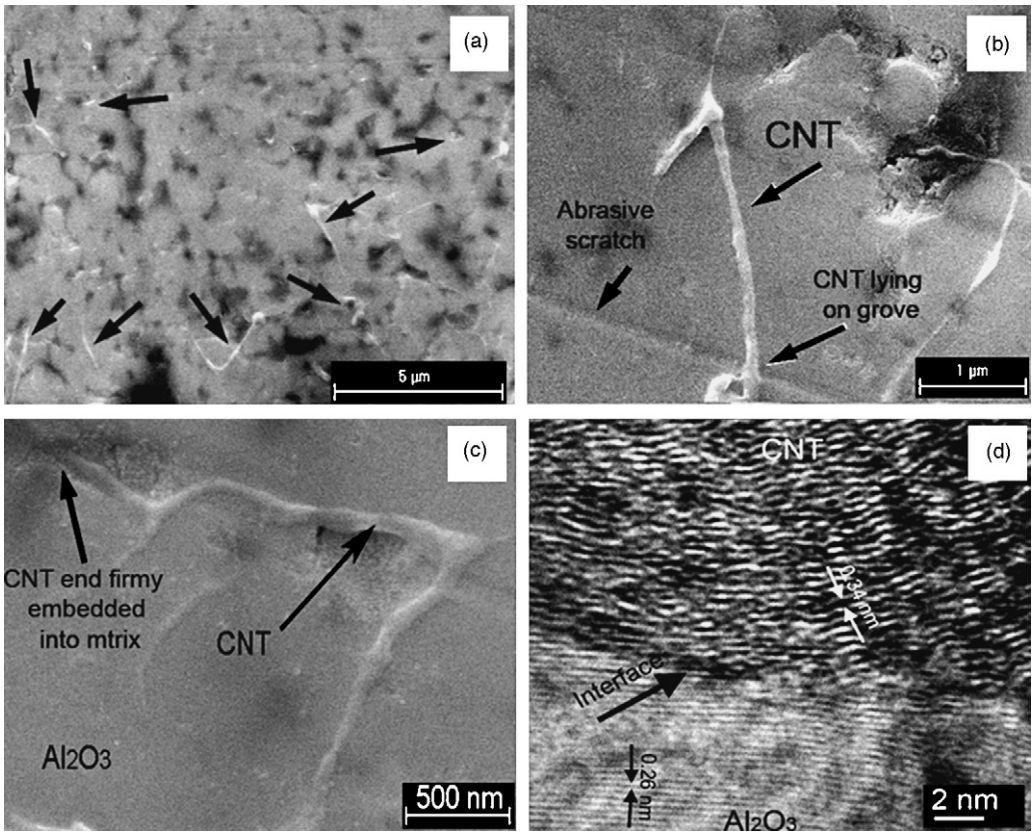

Fig. 9. (a) SEM image displays protruded MWCNTs on a nanocomposite worn surface (black arrows showing the MWCNTs), (b) and (c) individual MWCNT on a worn surface, and (d) high-resolution TEM image of the interfacial connection of Al_2O_3/MWCNT interface.

strengthened the grain boundaries via a pinning mechanism [26]. Furthermore, the presence of MWCNTs within the grains also acted as a barrier for cracks generated at worn surfaces, terminating further propagation inside the grains, via a crack bridging phenomenon [27].

Further observations revealed the abundance protruding MWCNTs on the worn nanocomposite surfaces, as shown in Fig. 9a. High-resolution SEM images (Fig. 9b and c) clearly show the MWCNT lying on a worn surface. It is apparent that one end of the MWCNT is laid flat on the worn surface, while the other end remains firmly embedded with the matrix, as shown in Fig. 9b and c. It is most likely that the exposed part of the MWCNT may act as a solid lubricant between the nanocomposites and the counter abrasive due to their inherent lubrication properties, and take the role as a rolling medium between the two surfaces minimising the wear [6,28]. Well-dispersed MWCNTs lead to nanocomposites with higher densities while agglomerated resulted in lower one [17]. Elimination of pores and mass transportation through bulk diffusion determine the final density of Al_2O_3 during sintering process. It is believed that too high additions of MWCNTs adversely affected these two important sintering parameters and led nanocomposites to lower densities, as already reported [17,29]. The high weight loss of 10 wt% MWCNT nanocomposites at 35 N load can be associated with the lower density and mechanical properties (Table 1), caused by the MWCNTs agglomerates as shown in Fig. 7. Some of the MWCNT agglomerates, although peeled off from the matrix, could remain embedded in matrix and act as a lubricant, as evidenced in Fig. 7a, therefore reduced the friction coefficient, as shown in Fig. 3b. It is striking that even under such severe conditions the MWCNTs maintain their tubular morphological characteristics, due to their unique tubular structure, nanoscale features and outstanding mechanical properties particularly the elasticity [30,31].

MWCNTs resistance to crumpling is evidenced in Fig. 9b, in which a MWCNT lies over a groove. It is possible that hard particles damaged the matrix and left the scratch, but leaving the MWCNTs unharmed. This could be explained due to rolling of the MWCNTs again abrasive debris [14]. To exploit such unique lubrication characteristics of MWCNTs, a strong interfacial connection between the matrix and the MWCNTs is essential in this context. As a weak interface connection with matrix would have ended up with MWCNTs being dragged out of the worn surface during wear, and losing their lubrication features and becoming debris. Our recent study has shown that the Al_2O_3 chemically reacted with the MWCNT via carbothermal reduction, and strong connection at the Al_2O_3/MWCNT interface was created as demonstrated in Fig. 9d where the MWCNT can be identified by its curved morphology and typical fringe separation of 0.34 nm which corresponds to the graphitic (0 0 2) planes of MWCNTs and Al_2O_3 can be identified by its fridge distance of 0.26 nm corresponds to (1 0 4) planes [32,33]. A close contact between Al_2O_3 and MWCNTs is clearly visible at the Al_2O_3/MWCNT interface. Thus, this desired strong interfacial connection makes it practical for the MWCNT's direct contribution towards the improved wear rates and reduced coefficient of friction.

4.3. Wear model

Based on the above discussions that involve the indirect role of MWCNTs via grain refining and a change in fracture mode illustrated in Figs. 2 and 6, and the direct contribution of MWCNTs to the reduced friction coefficient via a flattened distribution on the wear surface (Fig. 9), a schematic model has been proposed to describe the wear mechanism for the nanocomposites, as demonstrated in Fig. 10. In this model, a large grain size and inter-granular fracture features are dominant in monolithic Al_2O_3. During wear, surface cracks will originate from and concentrate at the grain boundaries,

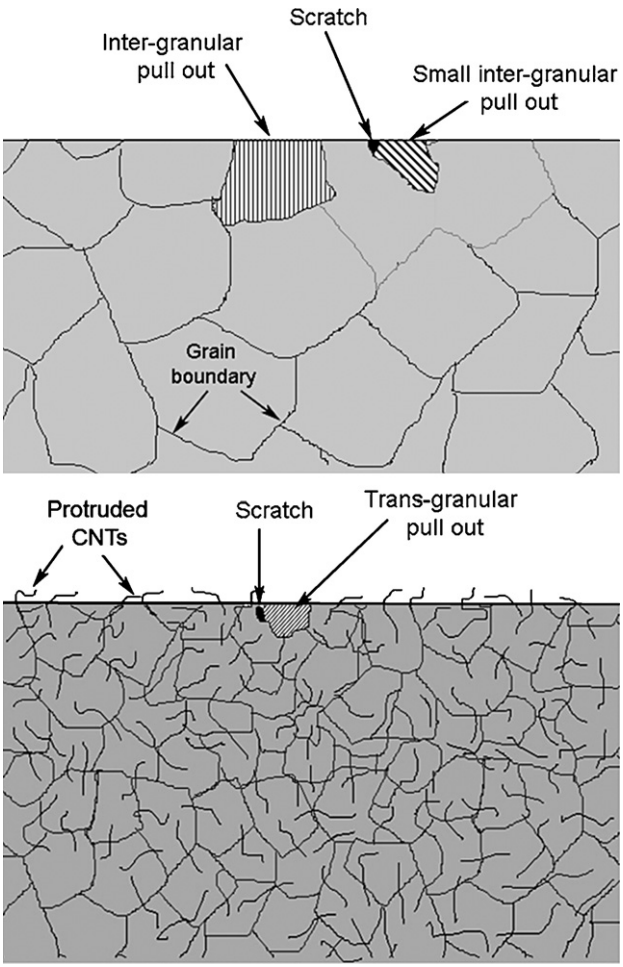

Fig. 10. Schematic wear mechanism for (a) monolithic Al_2O_3 and (b) Al_2O_3–MWCNT nanocomposite.

ultimately causing the pull-out of whole grains. In some cases, the crack path propagates across neighbouring grains which leads to much larger pull-outs, as shown in Fig. 10a. As for nanocomposites, the transgranular crack path is determined largely by the stress field around the scratches and hence, it is proposed that cracks propagating into the grains will quickly cease on the worn surface due to the smaller grain size [34,22]. As a result, relatively small pull-outs will occur, as displayed in Fig. 10b.

The MWCNTs also protrude from the worn surfaces and act as lubricious rollers between the sample and the hard debris or counterpart. The stiff nature and high strength enable the MWCNTs to survive abrasive wear and contribute to the improved resistance against wear. Finally, the presence of good interfacial connections, as presented in Fig. 9d, ensures the existences of MWCNTs on the nanocomposites surface and allows the direct contribution towards improved tribological performance and reduced coefficient of friction of the nanocomposites.

5. Conclusions

In this paper, the wear and tribological properties of hot-pressed Al_2O_3–MWCNT nanocomposites were investigated. Reduced coefficients of friction and improved wear resistance for the nanocomposites (reinforced with 2, 5 and 10 wt% MWCNTs) were obtained for low and moderate sliding loads; whilst for high sliding loads (35 N), the 10 wt% MWCNT nanocomposite exhibited lower wear resistance. The indirect and direct role of the MWCNTs in the

improved tribological properties of the Al_2O_3–MWCNT nanocomposites was discussed. These results showed that tough and highly wear resistant nanocomposites could be excellent candidates for a wide range of engineering applications.

Acknowledgements

IA thanks the Government of Pakistan and The University of Nottingham for scholarship support. YQZ thanks Marion Unwin, Alexander Kalashnikov, Hongzhi Cao, Huahui Chen, Huiyou Zhao, Keith Dinsdale and Thomas Buss for their technical help.

References

[1] E.V. Barrera, M.L. Shofner, E.L. Corral, in: M. Meyyappan (Ed.), Carbon Nanotubes in Science and Application, CRC Press, New York, 2004.
[2] P.J. Harris, Carbon nanotubes composites, Int. Mater. Rev. 49 (2004) 31–43.
[3] A.L. Vasiliev, P. Rosalia, N.P. Padture, Single-walled carbon nanotubes at ceramic grain boundaries, Scr. Mater. 56 (2007) 461–463.
[4] C. Laurent, A. Peigney, A. Rousset, Carbon nanotubes-Fe–Al_2O_3 nanocomposites. Part II: microstructure and mechanical properties of the hot-pressed composites, J. Eur. Ceram. Soc. 18 (1998) 2005–2013.
[5] H. Atsushi, Y. Nobuaki, Sliding friction properties of carbon nanotubes coatings deposited by microwave plasma deposition, Tribol. Int. 37 (2004) 893–898.
[6] N. Boris, B.S. Susan, Tribological properties of carbon nanotube bundles predicted from atomiostic simulations, Surf. Sci. 487 (2001) 87–96.
[7] J.P. Tu, Y.Z. Yang, L.Y. Wang, X.B. Zhang, Tribological properties of carbon nanotube reinforced copper composites, Tribol. Lett. 10 (2001) 225–228.
[8] N.P. Padture, Multifunctional composites of ceramics and single-walled carbon nanotubes, Adv. Mater. 21 (2009) 1767–1770.
[9] G. Yamamoto, M. Omori, T. Hashida, H. Kimura, A novel structure for carbon nanotubes reinforced alumina composites with improved mechanical properties, Nanotechnology 19 (2008) 315708.
[10] G. Zhan, J. Kuntz, J. Wan, K. Mukherjee, Single walled carbon nanotubes as attractive toughing agent in alumina based nanocomposites, Nat. Mater. 2 (2003) 38–42.
[11] R.W. Siegel, S.K. Chang, P.M. Ajayan, Schadler, Mechanical behaviour of polymer and ceramic matrix nanocomposite, Scr. Mater. 44 (2001) 2061–2064.
[12] T. Wie, Z. Fan, F. Wie, A new structure for multi-walled carbon nanotubes reinforced alumina nanocomposite with high strength and toughness, Mater. Lett. 62 (2008) 641–644.
[13] Q.M. Gong, Z. Li, B. Hu, J. Liang, Tribological properties of carbon nanotube doped carbon/carbon compsoites, Tribol. Int. 39 (2006) 937–944.
[14] J.W. An, D.H. You, D.S. Lim, Tribological properties of hot-pressed alumina–MWCNTs composites, Wear 225 (2003) 677–681.
[15] D.S. Lim, D.H. You, H. Jang, Effect of CNT distribution on tribological behaviour of alumina–CNT composites, Wear 259 (2005) 539–544.
[16] Y. Go, O. Mamoru, A. Koshi, Structural characterization and frictional properties of carbon nanotube/alumina composite prepared by precursor method, Mater. Sci. Eng. B 148 (2008) 265–269.
[17] I. Ahmad, A. Kennedy, H. Zhao, Y.Q. Zhu, Carbon nanotubes reinforced MgO-doped Al_2O_3 nanocomposites, in: Proceeding of ECCM13: 13th European Conference on Composite Materials, Stockholm, Sweden, 2008.
[18] F. Jinpeng, D. Zhao, J. Song, Preparation and microstructure of multi-walled carbon nanotubes-toughened Al_2O_3 composites, J. Am. Ceram. Soc. 89 (2) (2006) 750–753.
[19] T.K. Shen, P. Hing, Ultrasonic through-transmission method of evaluating the modulus of elasticity of Al_2O_3–ZrO_2 composite, J. Mater. Sci. 32 (1997) 6633–6638.
[20] G.R. Anstis, P. Chantikul, D.B. Marshall, A critical evaluation of indentation technique for measuring fracture toughness: I, direct crack method, J. Amer. Ceram. Soc. 64 (1981) 533–538.
[21] S. Sasaki, J.B. Pethic, Effects of surrounding atmosphere on micro-hardness and tribological properties of sintered alumina, Wear (2000) 204–208.
[22] F.C. Zhang, H.H. Luo, T.S. Wang, S.G. Roberts, R.I. Todd, Influence factors on wear resistance of two alumina matrix composites, Wear 265 (2008) 27–33.
[23] G. Evan, B.J. Hockey, R.W. Rice, The Science of Ceramics Machining and Surface Finishing, II. US Govt. Printing Office, 1979, pp. 1–14.
[24] L. Jose, M. Ortiz, R.I. Todd, Relationship between wear rate, surface pull-out and microstructure during abrasive wear of Alumina and Alumina/SiC nanocomposites, Acta Mater. 53 (2005) 3345–3357.
[25] Y.S. Wang, B.J. Hockey, S.M. Hsu, Wear transition in monolithic alumina and zirconia–alumina composites, Wear (1995) 156–164.
[26] S.H. Kim, Y.H. Kim, K. Niihara, S.W. Lee, Tribological properties of hot-pressed alumina silicon nitride nanocomposites, Adv. Technol. Mater. Mater. Proc. 6 (1) (2004) 17–22.
[27] E.L. Corral, J. Garary, E.V. Barrera, Engineering nanostructure for single-walled carbon nanotubes reinforced silicon nitride nanocomposites, J. Am. Ceram. Soc. 91 (2008) 3129–3137.
[28] L.C. Zhang, Novel behaviour of friction and wear of epoxy composites reinforced by carbon nanotubes, Wear 261 (2006) 806–811.
[29] M. Bengisu, Engineering Ceramics, Springer-Verlag, Berlin, 2001 (Chapter 4, p. 227).
[30] M.M.J. Treacy, T.W. Ebbessen, J.M. Gibson, Exceptionally high Young's modulus observed for individual carbon nanotubes, Nature 381 (1996) 678–680.
[31] M.H.G. Wichmann, K. Schulte, H.D. Wagner, On nanocomposite toughness, Composite Sci. Technol. 68 (2008) 329–331.
[32] I. Ahmad, A. Kennedy, Y.Q. Zhu, Carbon nanotubes reinforced alumina nanocomposites: mechanical properties and interfacial investigations, J. Comput. Sci. Technol. (2010), doi:10.1016/j.comscitech.2010.03.007.
[33] I. Ahmad, A. Kennedy, Y.Q. Zhu, Carbon nanotubes toughened aluminium oxide nanocomposites, J. Eur. Ceram. Soc. 30 (2010) 865–873.
[34] L. Alexander, R. Vasiliev, N.P. Poyota, Padture, Single-walled carbon nanotubes at ceramics grain boundary, Scr. Mater. 56 (2007) 461–463.